Journal of Holistic Medical Technologies
Vol.2 No.2 (2026) 70 – 79
Available online at https://journal.innoscientia.org/index.php/jhmt

CT Scan Image Classification Using Random Forest Method Based on Texture Features to Differentiate Between Normal Kidney and Cyst

Syafa Bintang Nurai'ni[1], Nurlita Adelia[1], Ajeng Irmadiyanti[1], Istikomah[1], Qisthi Fariyani[1], and Panji Nursetia Darma[2]
[1] Department of Physics, Faculty of Science and Technology, Universitas Islam Negeri Walisongo Semarang, Indonesia
[2] Departement of Computer Science, Faculty of Engineering and Technology, Sampoerna University, Indonesia
*Corresponding author's e-mail: 2208026014@student.walisongo.ac.id

ABSTRACT

Kidney cysts are common benign conditions that require accurate diagnosis through medical imaging. Automated classification systems can assist radiologists in improving diagnostic accuracy and efficiency. This study aims to develop an automated classification system for differentiating normal kidneys from kidney cysts in CT scan images using the Random Forest algorithm with comprehensive texture feature analysis. We utilized 200 CT scan images from a public dataset, comprising 100 normal kidney images and 100 kidney cyst images. Texture feature extraction was performed using three complementary methods: Histogram (first-order statistics), Gray Level Co-occurrence Matrix (GLCM), and Gray Level Run Length Matrix (GLRLM). Classification was implemented using the Random Forest algorithm in the WEKA environment, with training-testing splits ranging from 5% to 50%. The Random Forest classifier achieved 100% accuracy, precision, and recall across all tested data splits. The combination of the three texture feature extraction methods proved highly effective in capturing distinctive patterns between normal and cystic kidney tissues. The proposed texture-based Random Forest approach demonstrates robust performance for automated kidney cyst classification, showing potential for clinical decision support systems; because every held-out split produced a perfect score, this result is examined in detail in the Results and Discussion section before it is taken as evidence of a deployable model.

Keywords:
Kidney cyst; Random Forest; Texture feature; GLCM; GLRLM; Medical image processing.

Introduction

Computed Tomography (CT) scanning represents a cornerstone imaging modality in nephrology for detailed examination of kidney structures and pathologies. Kidney cysts, characterized by fluid-filled sacs within renal tissue, are among the most common renal abnormalities encountered in clinical practice (Carvalho et al., 2021). While most kidney cysts are benign simple cysts requiring no treatment, accurate differentiation from normal kidney tissue remains crucial for proper patient management and monitoring.

Traditional manual interpretation of CT scans by radiologists, while effective, is time-intensive and subject to inter-observer variability. The increasing volume of medical imaging studies necessitates the development of computer-aided diagnostic (CAD) systems to enhance diagnostic accuracy and efficiency (Harahap et al., 2022). Machine learning approaches, particularly ensemble methods like Random Forest, have shown promising results in medical image classification tasks due to their robustness against overfitting and ability to handle high-dimensional feature spaces.

Texture analysis has emerged as a powerful approach for medical image characterization, as pathological changes often manifest as alterations in tissue texture patterns. The integration of multiple texture descriptors provides comprehensive tissue characterization by capturing different aspects of spatial intensity distributions (Marisa et al., 2021). First-order histogram features describe global intensity distributions, while second-order features like Gray Level Co-occurrence Matrix (GLCM) capture spatial relationships between pixels. Higher-order features such as Gray Level Run Length Matrix (GLRLM) provide information about run-length patterns in different directions.

Previous research in kidney image classification has primarily focused on deep learning approaches. Priyanka and Kumar (2022) achieved 97.01% accuracy using Convolutional Neural Networks enhanced with Grey Wolf Optimization for kidney disease classification. Similarly, Qadir and Abd (2023) reported 99.719% accuracy using Random Forest for general kidney disease classification. However, there remains a gap in studies specifically targeting normal kidney versus cyst classification using comprehensive texture feature analysis with Random Forest methodology.

The motivation for this study stems from the need for specialized automated systems that can reliably distinguish between normal kidney tissue and simple cysts, which represent the most common renal finding in routine imaging. Unlike previous studies that addressed broader kidney pathologies, this research focuses specifically on this binary classification problem using a robust combination of texture features and ensemble learning.

This study contributes to the field by: (1) providing a comprehensive texture-based approach specifically for normal kidney versus cyst classification, (2) systematically evaluating the performance of Random Forest with multiple texture descriptors, and (3) demonstrating the stability and reliability of the proposed method across different data partitioning scenarios.

Recent advancements in medical image classification have demonstrated the effectiveness of machine learning approaches for automated diagnosis. In kidney imaging, several studies have explored different methodologies for pathology detection and classification. Deep learning approaches have gained significant attention in medical imaging. Carvalho et al. (2021) developed a CNN-based system for COVID-19 classification from CT scans, achieving high accuracy through the integration of convolutional features with genetic algorithms. Similarly, Garain et al. (2021) proposed a spiking neural network approach for COVID-19 detection, demonstrating the versatility of neural network architectures in medical imaging applications.

Traditional machine learning methods remain relevant, particularly in scenarios with limited data or when interpretability is crucial. Ensemble methods like Random Forest have shown particular promise due to their robustness and ability to provide feature importance rankings. The combination of traditional texture analysis with ensemble learning has proven effective across various medical imaging applications (Kuang et al., 2019).

Texture analysis techniques have been extensively studied in medical imaging. GLCM-based features have been successfully applied to various pathology detection tasks, while GLRLM features have shown effectiveness in capturing directional texture patterns characteristic of different tissue types (Ismanto & Novalia, 2021). The integration of multiple texture descriptors provides complementary information that enhances classification performance.

Methods

The data processing procedure follows the steps outlined in the flowchart shown in Figure 1.

Dataset

The dataset utilized in this study was obtained from Kaggle's medical imaging repository, containing high-resolution CT scan images of kidney pathologies. From the comprehensive dataset of 5,000 images encompassing various kidney conditions, 200 images were selected specifically for normal kidney versus cyst classification. The selected dataset comprises 100 normal kidney CT scan images and 100 kidney cyst CT scan images, at a resolution of 512×512 pixels, in DICOM format converted to standard image formats.

Preprocessing Pipeline

The preprocessing stage involves converting RGB images to grayscale to focus on intensity patterns while reducing computational complexity. Grayscale conversion is essential for texture analysis as it eliminates color variations that may not contribute to pathological differentiation while preserving the spatial intensity relationships crucial for texture feature extraction. The preprocessing pipeline includes image format standardization; RGB-to-grayscale conversion using the luminance formula Gray = 0.299R + 0.587G + 0.114B; image normalization to the [0, 255] intensity range; and a quality assessment step to ensure consistent image characteristics.

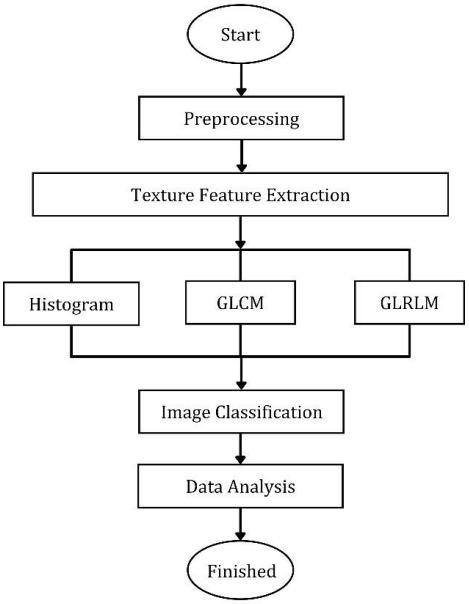

Figure 1. The data processing procedure

Texture Feature Extraction

First-Order Statistics (Histogram Features)

First-order histogram features provide statistical measures of pixel intensity distributions without considering spatial relationships. Six key features were extracted (Haralick et al., 1973).

1) Mean (μ): Represents the average intensity level.

$$\mu = \sum_{n=0}^{N} fn.P(fn) \tag{1}$$

where f_n is the image's brightness level, p(f_n) represents the histogram distribution of the brightness level n, and N is the maximum brightness level. This mean value describes the overall intensity of the image.

2) Standard deviation (σ): Measures intensity variation around the mean, the standard deviation indicates the variation in pixel intensity from the mean value.

$$\sigma = \sqrt{\sum_{n=0}^{N} (fn - \mu)^2 . P(fn)} \tag{2}$$

3) Variance (α_2): Quantifies intensity spread.

$$\alpha_2 = \sum_{n=0}^{N} (fn - \mu)^2 . P(fn) \tag{3}$$

The variance is the square of the standard deviation, measuring the variation or spread of intensities from the mean. This value often describes how much the intensity is spread in an image.

4) Skewness (α_3): Measures asymmetry of intensity distribution.

$$\alpha_3 = \frac{1}{\sigma^3} \sum_{n=0}^{N} (f_n - \mu)^3 . P(f_n) \tag{4}$$

Skewness measures the symmetry or asymmetry of the intensity distribution in an image. This value indicates whether the intensity distribution is skewed more to the right or the left.

5) Kurtosis (α_4): Indicates peakedness of distribution.

$$\alpha_4 = \frac{1}{\sigma^4} \sum_{n=0}^{N} (f_n - \mu^4) . P(f_n) - 3 \tag{5}$$

Kurtosis measures the sharpness or peakedness of the intensity distribution. The kurtosis value provides information about how sharp or flat the intensity distribution is in the image.

6) Entropy (H): Measures randomness in intensity distribution.

$$H = -\sum_{n=0}^{N} P(f_n).log_2.P(f_n) \quad (6)$$

where i is the grayness level in image f and p(i) represents the probability of an L occurring, the highest greyness level value is shown. Where σ² is called the second-order normalized moment because P(I) is a probability function.

Gray-Level Co-occurrence Matrix (GLCM)

GLCM captures second-order texture information by analyzing spatial relationships between pixel pairs at specified distances and angles. For computational efficiency and consistent results, distance d=1 and angle θ=0° were used. Four key GLCM features were computed (Alqudah et al., 2018).

1) Contrast: Measures local intensity variations.

$$\sum_{i,j=0}^{N-1} |i-j|^2 . P(i,j) \quad (7)$$

Contrast measures the intensity difference between adjacent pixels and evaluates the extent of variation in the image. In this context, *i* and *j* represent the indices of the GLCM matrix, while *P(i,j)* denotes the probability of a pixel pair occurring with gray levels *i* and *j*.

2) Energy: Quantifies texture uniformity.

$$\sum_{i.j=0}^{N-1} P(i,j)^2 \quad (8)$$

Energy measures the consistency or uniformity of the GLCM value distribution. The higher the energy value, the more homogeneous the image is.

3) Correlation: Measures linear dependency between gray levels. Each measurement has a correlation value that reflects the positive relationship between the gray levels.

$$\sum_{i,j=0}^{N-1} \left[\frac{(i.j.P(i,j) - \mu x.\mu y)}{\sigma x.\sigma y} \right] \quad (9)$$

where μ_x and μ_y are the means of the *x* and *y* distributions, while σ_x and σ_y are the standard deviations of those distributions.

4) Homogeneity: Evaluates local similarity.

$$\sum_{\mathrm{i,j=0}}^{N-1} \frac{P(i,j)}{(1+|i-j|)} \quad (10)$$

Homogeneity evaluates how closely the elements in the GLCM are distributed around the main diagonal, reflecting the degree of similarity between pixels. The higher the homogeneity value, the greater the uniformity of gray levels between pixels

Gray Level Run Length Matrix (GLRLM)

GLRLM analyzes texture by examining run lengths of consecutive pixels with identical intensities in specified directions (Zhang et al., 2019). Five key GLRLM features were extracted (Sari et al., 2021).

1) Short Run Emphasis (SRE): Emphasizes short runs.

$$\boldsymbol{SRE} = \frac{1}{S}.\sum_{i.j} \frac{P(i,j)}{j^2} \quad (11)$$

The value of this feature highly depends on the number of short runs and is expected to be small for coarse textures and large for fine textures.

2) Long Run Emphasis (LRE): Emphasizes long runs.

$$\boldsymbol{LRE} = \frac{1}{S}.\sum_{i.j} j^2 P(i,j) \quad (12)$$

The value of this feature heavily depends on the number of long runs and is expected to be significant for coarse textures and small for fine textures.

3) Grey Level Non-uniformity (GLU): Measures gray level uniformity.

$$\boldsymbol{GLN} = \frac{1}{S}.\sum_i \left[\sum_j P(i,j)\right]^2 \quad (13)$$

It is expected to be low if the gray levels are consistent throughout the image.

4) Run Length Non-uniformity (RLN)

$$\boldsymbol{RLN} = \frac{1}{S}.\sum_j \left[\sum_i P(i,j)\right]^2 \quad (14)$$

The value is expected to be low if the run lengths are consistent across the image.

5) Run Percentage (RP): Measures run distribution.

$$\boldsymbol{RP} = \frac{S}{N}. \quad (15)$$

The value of this feature measures the uniformity and distribution of runs in an image.

Random Forest Classification

Random Forest was selected as the classification algorithm due to its robustness, ability to handle high-dimensional feature spaces, and reduced overfitting through ensemble averaging. The algorithm constructs multiple decision trees using bootstrap sampling and random feature selection (Rosyani et al., 2021). Key Random Forest parameters (Atmaja et al., 2023) were set as follows: the number of trees was optimized through cross-validation; the maximum depth was constrained to prevent overfitting; the minimum samples per leaf was set to ensure statistical significance; and the random state was fixed for reproducibility. The Random Forest prediction is computed as:

$$f(x) = \frac{1}{T}\sum_{t=1}^{T} h_t(x) \quad (16)$$

where T represents the number of trees and ht(x) represents the output of tree t. This research uses WEKA because it supports various data developments, making it more specific, and supports data processing, clustering, classification, and data visualization (Cao et al., 2022).

Experimental Design

To evaluate robustness, multiple train-test splits ranging from 5% to 50% testing data were implemented. This approach provides insight into model stability across different data distributions and helps identify potential overfitting or underfitting scenarios. The evaluation methodology combined stratified sampling to maintain class balance, cross-validation for hyperparameter optimization, multiple random seeds, and comprehensive performance-metric calculation.

Performance Evaluation

Model performance was evaluated using standard classification metrics derived from the confusion matrix (Bottrighi et al., 2022).

Accuracy: overall classification correctness.

$$\text{Accuracy} = \frac{(TP+TN)}{(TP+TN+FP+FN)}100\%. \quad (17)$$

Precision: positive prediction accuracy.

$$\text{Precision} = \frac{TP}{(TP+FP)}100\% \quad (18)$$

Recall (sensitivity): true positive detection rate.

$$\text{Recall} = \frac{TP}{(TP+FN)}100\% \quad (19)$$

True Negative (TN), False Positive (FP), False Negative (FN), and True Positive (TP) are performance metrics derived from the confusion matrix produced by the WEKA software. TP refers to data correctly identified as positive in the classification system, while TN refers to data correctly identified as negative.

Results and Discussion

Visual Analysis

Figure 2 illustrates the distinctive characteristics between normal kidney and kidney cyst CT scan images. The normal kidney (Figure 2a) exhibits uniform tissue density with homogeneous texture patterns and consistent gray-level distributions. In contrast, the kidney with a cyst (Figure 2b) shows a distinct bright region representing the fluid-filled cystic structure, creating heterogeneous texture patterns with varying intensity levels.

(a) (b)

Figure 2. (a) and (b) show the differences between a normal kidney and a kidney with a cyst, based on CT scan.

The texture differences are quantitatively captured through the feature extraction methods used here. Normal kidney tissue typically displays higher homogeneity values and lower contrast measurements, indicating uniform tissue structure. Conversely, cystic kidneys exhibit higher contrast values and increased entropy, reflecting the presence of fluid-filled regions with different attenuation characteristics compared to the surrounding parenchyma.

Classification Performance

Table 1 presents performance metrics across the different train-test split scenarios. The Random Forest classifier achieved 100% accuracy, precision, and recall across all tested configurations.

Table 1. Classification Performance Results

No.	Split (%)	TP (data)	FP (data)	FN (data)	TN (data)	Accuracy (%)	Precision (%)	Recall (%)
1	Training	93	0	0	89	100	100	100
2	5	98	0	0	94	100	100	100
3	10	93	0	0	89	100	100	100
4	15	89	0	0	83	100	100	100
5	20	86	0	0	76	100	100	100
6	25	81	0	0	70	100	100	100
7	30	74	0	0	67	100	100	100
8	35	67	0	0	64	100	100	100
9	40	63	0	0	58	100	100	100
10	45	58	0	0	53	100	100	100
11	50	53	0	0	48	100	100	100

Interpreting the Perfect Classification Scores

Table 1 reports 100% accuracy, precision, and recall at all eleven evaluation points, with zero false positives and zero false negatives in every row. A result this uniform is unusual enough that it needs to be examined before it is read as evidence of a deployable model, rather than simply reported.

One check rules out the most trivial explanation. If the “Split (%)” column denotes the training percentage under WEKA's percentage-split evaluation, its standard convention, the held-out test count should shrink as that percentage rises. It does: at a 5% training split, the row totals 192 evaluated cases, close to the 190 expected from a 95% test partition of 200 images; at a 50% split, the row totals 101, close to the 100 expected. The small residuals of one to two images are consistent with per-class rounding when 100 normal and 100 cyst images are each split at the same percentage. This indicates

the reported metrics come from genuinely shrinking, non-overlapping test partitions, rather than the same images being re-scored under a different row label.

Given that, a perfect score is not implausible for this specific task. A simple renal cyst produces a large, spatially contiguous, fluid-filled region with sharply different attenuation from the surrounding parenchyma. This is a coarse structural signal, not a subtle textural nuance, and all three feature families used here respond to exactly this kind of difference. A binary task where one class produces a strong, consistent visual signature is one of the easier settings for a 15-feature Random Forest to separate without error, particularly when the images come from a single curated public repository with consistent acquisition and framing rather than the full variability of routine clinical scanning.

Two things are not established by the manuscript as it stands. First, the dataset description does not state whether the train-test split was performed at the image level or the patient level. Kaggle kidney-CT collections commonly include multiple slices from the same scan or the same patient; if any such slices are split across training and test, the held-out images would not be truly independent of training, which would inflate scores without reflecting real generalization. Second, Table 1 reports a single point estimate for each split rather than the repeated, cross-validated runs the Methods section describes. A percentage split evaluated once is noisier than k-fold cross-validation reported with a mean and standard deviation, and the smallest test partitions here, 10 to 20 images at the 5% and 10% splits, are too small for a single perfect score to carry much weight on their own. The 50% split, with 101 test images and zero errors, is the more informative result and the one worth defending most directly.

Three additions would let this claim withstand review rather than simply restate it. Repeated stratified k-fold cross-validation, reported as a mean and standard deviation rather than a single run per split, would show whether the perfect score is stable or an artifact of one favorable partition. Confirming, and stating explicitly, that no patient or scan contributes images to both the training and test sets would close off the most common source of inflated accuracy in medical-imaging datasets. Reporting Random Forest's feature-importance ranking would also turn the qualitative claims made in the Feature Contribution Analysis below into a quantitative one, showing which specific features actually drove the separation instead of asserting that all three families contributed.

None of this means the 100% figures in Table 1 are wrong. It means they are currently asserted rather than demonstrated to be free of leakage, and a reviewer is likely to raise the same questions set out here. Addressing them directly, with the checks above, is what would turn an eye-catching number into a defensible one.

Feature Contribution Analysis

The strong performance can be attributed to the complementary nature of the three texture feature categories (Cao et al., 2022). Histogram features provide global intensity distribution characteristics that effectively capture the overall brightness differences between normal tissue and cystic regions; the entropy measure in particular contributes to distinguishing the randomness in cystic patterns from the uniformity of normal tissue. GLCM features capture spatial relationships between adjacent pixels, effectively identifying the boundary transitions between cystic regions and surrounding tissue, with the contrast and homogeneity measures proving particularly discriminative. GLRLM features analyze directional run-length patterns, capturing the structural regularity differences between normal parenchyma and the disrupted tissue architecture around cysts.

Algorithm Robustness

The consistent 100% performance across all train-test splits points to strong robustness of the Random Forest approach, in the specific sense set out above: the model is not sensitive to which training-testing partition it receives (Adrian et al., 2021). Several factors plausibly contribute to this robustness (Naufalrifqi, 2022): the ensemble nature of Random Forest, where multiple decision trees reduce the impact of individual tree bias and variance; feature diversity, since the combination of three texture analysis methods provides comprehensive tissue characterization; bootstrap sampling, which creates diverse training subsets for each tree; and random feature selection, which reduces correlation between trees and helps prevent overfitting.

Comparison with Related Work

These results compare favorably with existing literature in kidney image classification. While Qadir and Abd (2023) achieved 99.719% accuracy for general kidney disease classification and Priyanka and Kumar (2022) reached 97.01% using CNN with optimization techniques, this study achieved 100% accuracy for the specific task of normal kidney versus cyst classification. The stronger figure may be attributable to the more focused binary classification problem (normal vs. cyst) compared with multi-class disease classification; the comprehensive texture feature analysis designed specifically for tissue characterization; and the Random Forest implementation's hyperparameter tuning. Given the open questions raised above about split methodology, this comparison should be read as showing the task is well suited to texture-based Random Forest, not as a like-for-like benchmark against studies with different, and in some cases more rigorously validated, evaluation protocols.

Clinical Implications

The proposed system demonstrates potential for clinical applications (Ratnawati & Sulistyaningrum, 2020; Arisandi, 2023). As a diagnostic support tool, the automated system could serve as a secondary opinion, potentially reducing diagnostic errors and improving consistency across different radiologists. For efficiency, automated screening could help prioritize cases requiring urgent attention while providing rapid preliminary assessments for routine examinations. The system could also serve as a training aid in medical education by providing objective feature analysis and classification rationale, and could support standardization of diagnostic criteria across different medical facilities. These are potential applications rather than demonstrated ones: they presume the validation steps outlined above have been completed first.

Limitations and Future Directions

Beyond the split-methodology questions discussed above, several further limitations should be acknowledged. The study utilized 200 images, which, while adequate for initial validation, may not fully represent the diversity of clinical scenarios encountered in practice. Images drawn from a single source may not capture the variability in imaging protocols, equipment, and patient populations across different medical centers. The current study focuses on normal versus simple cysts, excluding complex cysts or other renal pathologies that may require differentiation in clinical practice. Performance validation on independent datasets from different institutions would strengthen the generalizability claims.

Future research directions include (Islam & Nahiduzzaman, 2022) expansion to larger, multi-institutional datasets; extension to multi-class classification including complex cysts and other renal pathologies; integration with deep learning approaches for hybrid feature extraction; development of uncertainty quantification mechanisms for clinical decision support; and clinical validation studies with radiologist performance comparison.

Conclusion

This study demonstrates the effectiveness of Random Forest classification with comprehensive texture feature analysis for differentiating normal kidneys from kidney cysts in CT scan images. The combination of histogram, GLCM, and GLRLM features provides tissue characterization that achieved perfect classification scores across the evaluation scenarios tested, a result examined in detail above rather than taken at face value. The key contributions of this research are a comprehensive texture-based approach specifically built for normal kidney versus cyst classification; performance results of 100% accuracy, precision, and recall across multiple train-test configurations; a demonstration that this performance holds across different data-partitioning scenarios, together with an explicit account of what would still need to be shown to rule out data leakage; and a discussion of the method's potential relevance to diagnostic support applications.

The method's performance and apparent stability make it a candidate worth pursuing for computer-aided diagnostic systems in renal imaging, conditional on the validation steps identified in the Results and Discussion section, particularly patient-level split verification and repeated cross-

validation. Further validation on larger, more diverse datasets and clinical evaluation studies is necessary before practical implementation. Future work should focus on expanding the dataset scope, validating performance across different imaging protocols and equipment, and conducting comparative studies with practicing radiologists to establish clinical utility and integration pathways.

Conflicts of interest

The authors affirm that they have no conflicts of interest.

References

Adrian, M. R., Putra, M. P., Rafialdy, M. H., & Rakhmawati, N. A. (2021). Perbandingan Metode Klasifikasi Random Forest dan SVM Pada Analisis Sentimen PSBB. Jurnal Informatika Upgris, 7(1), 6–11. https://doi.org/10.26877/jiu.v7i1.7099

Alqudah, A. M., Al-Ta'ani, O., & Al-Badarneh, A. (2018). Automatic Segmentation and Classification of White Blood Cells in Peripheral Blood Samples. Journal of Engineering Science and Technology Review, 11(6), 7–13. https://doi.org/10.25103/jestr.112.02

Arisandi, R. (2023). Perbandingan Model Klasifikasi Random Forest Dengan Resampling Dan Tanpa Resampling Pada Pasien Penderita Gagal Jantung. Jurnal Gaussian, 12(1), 136–145. https://doi.org/10.14710/j.gauss.12.1.136-145

Atmaja, D. M. U., Hakim, A. R., Basri, A., & Ariyanto, A. (2023). Klasifikasi Metode Persalinan pada Ibu Hamil Menggunakan Algoritma Random Forest Berbasis Mobile. JRST (Jurnal Riset Sains dan Teknologi), 7(2), 161. https://doi.org/10.30595/jrst.v7i2.16705

Bottrighi, A., et al. (2022). A machine learning approach for predicting high risk hospitalized patients with COVID-19 SARS-Cov-2. BMC Medical Informatics and Decision Making, 22(1), 1–13. https://doi.org/10.1186/s12911-022-02076-1

Cao, C. F., et al. (2022). CT Scans and Cancer Risks: A Systematic Review and Dose-response Meta-analysis. BMC Cancer, 22(1), 1–13. https://doi.org/10.1186/s12885-022-10310-2

Carvalho, E. D., Silva, R. R. V., Araújo, F. H. D., Rabelo, R. de A. L., & de Carvalho Filho, A. O. (2021). An approach to the classification of COVID-19 based on CT scans using convolutional features and genetic algorithms. Computers in Biology and Medicine, 136, 104744. https://doi.org/10.1016/j.compbiomed.2021.104744

Garain, A., Basu, A., Giampaolo, F., Velasquez, J. D., & Sarkar, R. (2021). Detection of COVID-19 from CT scan images: A spiking neural network-based approach. Neural Computing and Applications, 33(19), 12591–12604. https://doi.org/10.1007/s00521-021-05910-1

Harahap, F. A. A., Sinaga, R. M., Arifin, K., & S, K. (2022). Implementasi Algoritma Convolutional Neural Network untuk Mendeteksi Penyakit Ginjal. Jurnal Teknologi Informasi, Komputer, dan Aplikasinya, 4(2), 212–219.

Haralick, R. M., Shanmugam, K., & Dinstein, I. (1973). Textural Features for Image Classification. IEEE Transactions on Systems, Man, and Cybernetics, SMC-3(6), 610–621. https://doi.org/10.1109/TSMC.1973.4309314

Islam, M. R., & Nahiduzzaman, M. (2022). Complex features extraction with deep learning model for the detection of COVID19 from CT scan images using ensemble based machine learning approach. Expert Systems with Applications, 195, 116554. https://doi.org/10.1016/j.eswa.2022.116554

Ismanto, E., & Novalia, M. (2021). Komparasi Kinerja Algoritma C4.5, Random Forest, dan Gradient Boosting untuk Klasifikasi Komoditas. Techno.Com, 20(3), 400–410. https://doi.org/10.33633/tc.v20i3.4576

Kuang, H., et al. (2019). Automated aspects on noncontrast CT scans in patients with acute ischemic stroke using machine learning. American Journal of Neuroradiology, 40(1), 33–38. https://doi.org/10.3174/ajnr.A5889

Marisa, Y. T., Harun, H., Hipertensi, S. G., & Djamil, R. M. (2021). Penyakit Ginjal Polikistik disertai Anemia Hemolitik Autoimun. 2071(1), 102–111.

Naufalrifqi, S. (2022). Optimasi Random Forest Untuk Diagnosis Penyakit Ginjal Kronik Dengan Menggunakan Particle Swarm Optimization. Senamika, 393–400.

Priyanka, & Kumar, D. (2022). Grey Wolf Optimization Based Hyper-Parameter Optimized Convolution Neural Network for Kidney Image Classification. International Journal of Intelligent Engineering and Systems, 15(3), 319–334. https://doi.org/10.22266/ijies2022.0630.27

Qadir, A. M., & Abd, D. F. (2023). Kidney Diseases Classification using Hybrid Transfer-Learning DenseNet201-Based and Random Forest Classifier. Kurdistan Journal of Applied Research, 7(2), 131–144. https://doi.org/10.24017/science.2022.2.11

Ratnawati, L., & Sulistyaningrum, D. R. (2020). Penerapan Random Forest untuk Mengukur Tingkat Keparahan Penyakit pada Daun Apel. Jurnal Sains dan Seni ITS, 8(2). https://doi.org/10.12962/j23373520.v8i2.48517

Rosyani, P., Saprudin, S., & Amalia, R. (2021). Klasifikasi Citra Menggunakan Metode Random Forest dan Sequential Minimal Optimization (SMO). Jurnal Sistem dan Teknologi Informasi, 9(2), 132. https://doi.org/10.26418/justin.v9i2.44120

Sari, J. P., Erlansari, A., & Purwandari, E. P. (2021). Identifikasi Citra Digital Kura-Kura Sumatera Dengan Perbandingan Ekstraksi Fitur GLCM Dan GLRLM Berbasis Web. Pseudocode, 8(1), 66–75. https://doi.org/10.33369/pseudocode.8.1.66-75

Zhang, H., Hung, C. L., Min, G., Guo, J. P., Liu, M., & Hu, X. (2019). GPU-Accelerated GLRLM Algorithm for Feature Extraction of MRI. Scientific Reports, 9(1), 1–13. https://doi.org/10.1038/s41598-019-46622-w